



# STRUCTURAL AND THERMOELECTRIC POWER PROPERTIES OF GADOLINIUM DOPED MANGANESE CADMIUM NANOFERRITES

Srilata Michael<sup>1</sup>, Dr. D. Ravinder<sup>a</sup>

1 Research Scholar, Department of Physics, Osmania University, Hyderabad, Telangana, India. 500007.

Professor (Retd.) Department of Physics, Osmania University, Hyderabad, Telangana, India. 500007.

**Abstract :** The nano ferrite chosen for thermoelectric power studies is Manganese cadmium ferrite which is doped with gadolinium, a rare earth element and the composition of the compound is  $\text{Mn}_{0.3}\text{Cd}_{0.7}\text{Gd}_x\text{Fe}_{2-x}\text{O}_4$  where  $x$  takes the values of 0.000, 0.005, 0.010, 0.015, 0.020 and 0.025 and the compound is synthesized using citrate gel auto combustion method at a lower processing temperature of  $180^\circ\text{C}$  and in this process of synthesis citric acid is used as fuel and as an oxidant. For the analysis of the structure of the samples the characterization techniques used are XRD analysis, FTIR spectroscopy, Transmission electron microscopy (TEM), EDAX, SEM micrographs analysis. The homogeneous single phase cubic spinel structure of the samples that were prepared and sintered was confirmed from the XRD analysis and the crystallite sizes were found to range from 32 to 36 nm. The spinel ferrites were found to possess properties that include high resistivity, low dielectric losses, high Curie temperature, considerable magnetic properties, thermoelectric power and many other that makes them useful in many applications. [1][2] From the graphs of wave number versus Transmission, plotted from the data of FTIR, it was observed that the two significant absorption bands have appeared in the range of  $500$  to  $400\text{ cm}^{-1}$  and the vibrations of tetrahedral complexes and octahedral complexes in the high frequency band and the low frequency band confirmed the existence of double and triple bonds in the fingerprint region of the FTIR spectroscopic graphs. TEM images confirmed the formation of nano sized particles and agglomeration of the particles with an average particle size of 28-30 nm. Further the SAED analysis confirmed the polycrystalline nature of the prepared samples and the orientation relationships that describe how the atomic arrangements in neighboring grains or phases are oriented relative to each other in the crystal were identified. As part of analysis of electrical properties of the prepared samples thermoelectric power studies was undertaken using Seebeck effect in differential method. The variation of Seebeck coefficient with the temperature has been studied and the transition temperature

has been noted for all the samples with increasing doping concentration of Gadolinium. This transition temperature of the prepared samples was measured and its variation with the doping concentration has been noted. The p type and the n type semiconductor nature of the prepared samples is studied. The energy band gap and carrier concentration is determined and this behavior can be used in Thermoelectric generators, Industrial waste recovery, automotive exhaust heat recovery, Thermoelectric coolers used for CPUs, Medical devices, aerospace applications, sensors. [3][4]

keywords: XRD analysis, FTIR analysis, FESEM analysis, TEM analysis, HRTEM analysis, Seebeck coefficient and Thermoelectric power.

**Introduction** Nano ferrites belonging to soft ferrite category and in its oxide form have become a considerable topic under research and gained popularity in its synthesis worldwide. These materials gained importance due to nanotechnology which revolutionized the material science where in these materials are used in nanotechnology as the basic components. To work towards the objective set, the samples of Gd doped  $\text{Mn}_{0.3}\text{Cd}_{0.7}\text{Gd}_x\text{Fe}_{2-x}\text{O}_4$  with  $x=0.00, 0.005, 0.010, 0.015, 0.020, 0.025$  are prepared through citrate gel auto combustion method and sintered at temperatures of  $750^\circ\text{C}$ . Using XRD, FTIR, TEM, FESEM and SAED analysis, the polycrystalline, homogeneous, cubic structure of the nano ferrites synthesized was confirmed. Further to investigate the electrical conductivity of the samples, and hence the thermo electric power, the method used is differential method in the temperature range of  $100^\circ\text{C}$  -  $650^\circ\text{C}$ . [4]

**Results and discussion:** Using XRD analysis, the average crystallite size of the prepared samples was calculated using Debye- Scherrer's formula

$$D = 0.91\lambda / \beta \cos\theta \text{-----(1)}$$

where D stands for the crystallite size in nm,  $\lambda$  is the wave length of the X-rays used ( $1.5405 \text{ \AA}$ ),  $\beta$  is the full width half maximum (FWHM) and ' $\theta$ ' is the diffraction angle in radians.

The lattice constant 'a' is calculated using the formula,  $a = d\sqrt{h^2 + k^2 + l^2}$  \_\_\_\_\_ (2)

Where 'd' is the inter planer spacing which is obtained from the Bragg's equation,  $n\lambda = 2d\sin\theta$

And  $d = n\lambda / 2\sin\theta$  where  $n=1, 2, 3, \dots$ ,  $\lambda$  is the wave length of the X-rays used ' $\theta$ ' is the angle of diffraction. h, k, l are the miller indices. The hopping lengths are calculated using the following relations for tetrahedral site ( $d_A$ ) and for octahedral site ( $d_B$ ) which are

$$d_A = 0.25 a\sqrt{3} \text{ _____ (3a)}$$

$$d_B = 0.25 a\sqrt{2} \text{ _____ (3b)}$$

The X-ray density,  $\rho_x$ , was calculated by using the following formula,

$$\rho_x = nM/a^3N \text{----- (4)}$$

where n is the number of molecules in a unit cell of spinel lattice ( $n=8$ ), M is the molecular weight of the sample and N is the Avagadro number ( $6.023 \times 10^{23}$  molecules/cc).

The Bulk density,  $\rho_B$  is calculated by using the formula,

$$\rho_B = m / \pi r^2 t \text{----- (5)}$$

where m is the mass of the pellet, r is the radius of the pellet and t is the thickness of the pellet.

The porosity of the sample is determined from the relation ,

$$P = (d_x - d_B / d_x) \times 100 \text{----- (6) where } d_x \text{ is the x-ray density and } d_B \text{ is the bulk density.}$$

The procedure followed for the study of thermo electric power involves making a pellet form of the sample prepared using hydraulic press and then the pellet is coated with silver paint on both of its surfaces and heated on a hot plate for making it to have a good electrical contact. The pellete thus prepared is placed between two electrodes of a specially designed sample holder and placed in a heater controlled by a thermostat and another thermostat is connected to the other electrode and thus a temperature difference of about 10K is maintained between the two electrodes and the voltage developed is recorded by the nano micro volt meter[5][6]. The thermo electric power or seebeck coefficient (s) is calculated using the following formula

$$S = \Delta V / \Delta T \text{----- (} \mu\text{V/K)} \text{----- (7)}$$

Where  $\Delta V$  is the thermo e.m.f produced across the two ends of the sample and  $\Delta T$  is the difference in temperature between the two surfaces of the pellet.

The energy band gap,  $E_g$  can be estimated using the Seebeck coefficient,  $S$  and Temperature,  $T_c$  from the given formula, [19] ,  $E_g = 2eST$ ----- (8) Where  $e$  is the electronic charge equal to  $1.602 \times 10^{-19} \text{C}$

The carrier concentration values of the samples is determined using the following relation,  $n = 2N_c \exp(E_g / 2k_B T)$  ----- (9) Where  $N_c = 10^{19} / \text{cm}^3$  which is the effective density of states in the conduction band,  $k_B$  is Boltzmann's constant

The results of structural/microstructural, thermo electric power studies of the samples so prepared is being discussed below .

**XRD studies:** Fig(1) shows the XRD plots drawn for intensity vs diffraction angle of the samples that were prepared. The XRD plots revealed the formation of a single -phase cubic spinel structure and the data is confirmed by comparing the same with the reference data from JCPDS card number. The XRD patterns confirmed the basic crystal structure of the prepared samples. The obtained P-XRD patterns of all Gd samples show a highly pure, single-phase spinel crystal structure. The existence of characteristic peaks at 18.24, 30.24, 35.65, 37.25, 43.22, 53.60, and 57.16 correspond to the (111) (220), (311), (222), (400), (422), (511), and (440) are considered as main lattice planes in the P-XRD patterns, which provides evidence for the development of spinel structure with Fd-3m space group. [8][11][12] Table 1. Structural parameters : crystallite size (D), lattice parameter (a), Volume (V), X-ray density ( $d_x$ ), bulk density ( $d_B$ ), and percentage porosity (P%), for the synthesized Gd doped MnCd nanoferrite for various compositions of x

x	FWHM	D (nm)	D- Spacing	a Å	LA	LB	$d_x$	$d_B$	Volume	P%
Gd-0 (0.000)	0.2614	31.95	2.4952	8.3007	3.5943	2.9348	6.29123	3.164	571.938	43.964
Gd-1 (0.005)	0.2562	32.60	2.4996	8.3154	3.6007	2.9399	6.01948	3.061	574.975	40.492
Gd-2 (0.010)	0.2483	33.62	2.5046	8.3320	3.6079	2.9458	6.25023	3.112	578.428	39.580

Gd-3 (0.015)	0.2433	34.30	2.5104	8.3510	3.6161	2.9526	6.26307	3.145	582.410	39.014
Gd-4 (0.020)	0.2340	35.66	2.5171	8.3734	3.6258	2.9605	6.27574	3.158	587.099	38.796
Gd-5 (0.025)	0.2287	36.48	2.5235	8.3946	3.6350	2.9680	6.29097	3.162	591.568	38.741

In the figure given below it must be noted that Gd-0 refers to the compound with  $x=0.000$ , Gd-1 refers to the compound with  $x=0.005$ , Gd-2 refers to the compound with  $x=0.010$ , Gd-3 refers to the compound with  $x=0.015$ , Gd-4 refers to the compound with  $x=0.020$ , Gd-5 refers to the compound with  $x=0.025$ ,

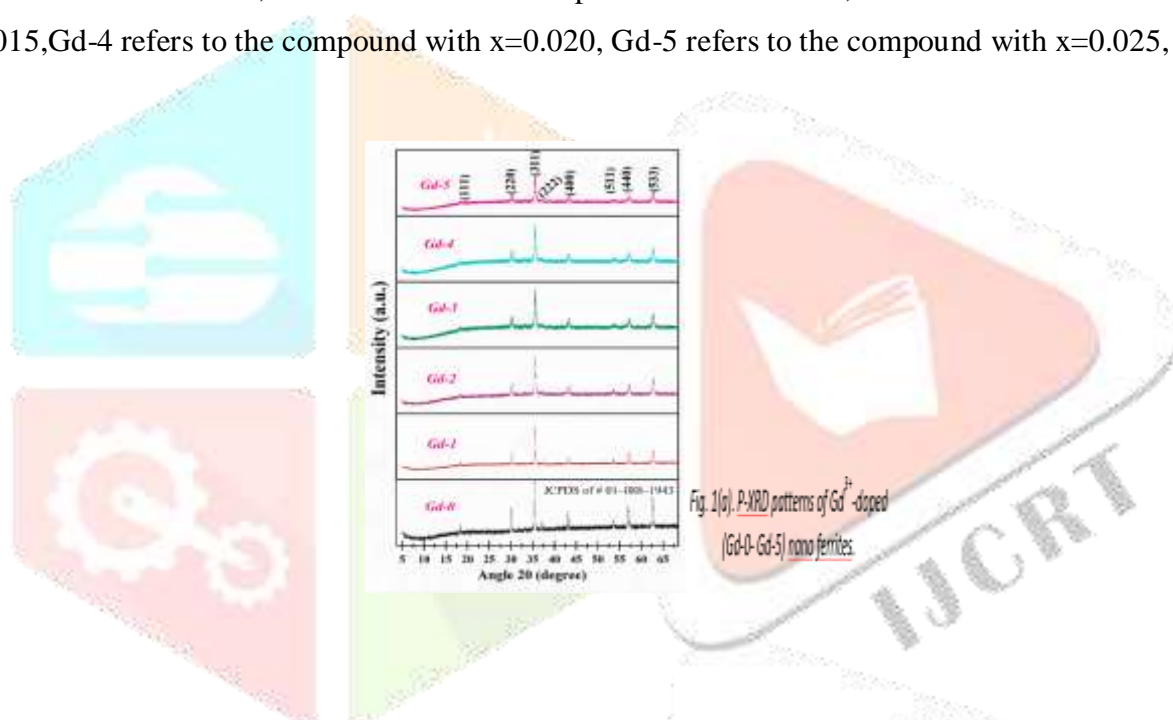


Fig. 1(a). XRD patterns of Gd<sup>3+</sup>-doped (Gd-0-Gd-5) nano ferrites.

From the table 1, it is observed that the lattice constant,  $a$  of the samples increases with the increase in the doping concentration and this can be attributed to the replacing of  $\text{Fe}^{3+}$  ions by  $\text{Gd}^{3+}$  ions as the former is larger in size than the latter. It is also observed that the average crystallite size of the samples that were prepared  $\text{Mn}_{0.3}\text{Cd}_{0.7}\text{Gd}_x\text{Fe}_{2-x}\text{O}_4$  of different compositions and calculated using Debye-scherrer's formula was found in the range of 32-36nm. The other crystal parameters that include lattice parameter also found to increase with the increase in the concentration of doping and obeys Vegard's law.

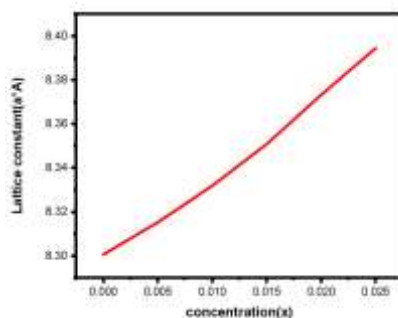


Fig.1(b) Graph using Vegard's Law

From the above graph it is observed that as the doping concentration is increased the lattice parameter also increases. The law assumes a linear relationship between the lattice parameter and the composition.

The hopping lengths that were calculated using equations (3a) and (3b) were found to increase as hopping length is directly proportional to 'a' the increase in the lattice constant is due to the larger ionic radius of  $Gd^{3+}$  ion ( $0.91 \text{ \AA}$ ) compared to those of  $Mn^{3+}$  ion and  $Fe^{3+}$  ion ( $0.64 \text{ \AA}$ ) [12] where in the substitution of  $Fe^{3+}$  ions by  $Gd^{3+}$  results in the increase in the size of the lattice.

The surface particle size of the pure and Gd-doped ferrite sample was approximately estimated to be between 22.23-34.26 nm, which is in close agreement with the crystallite size ( $D_{P-XRD}$ ) value found through P-XRD analysis (Scherrer's method) for the same sample. The observed average grain size proved the nanocrystalline structure of the prepared samples.

**FESEM & EDAX ANALYSIS:** Field Emission Scanning Electron Microscopy is a high resolution imaging characterization technique that is used to study the surface morphology and composition of materials. FESEM uses a focussed beam of electrons to scan the surface of the chosen samples thereby producing a high resolution images and spectroscopic data which are analyzed to extract information about the sample's surface morphology, composition and properties. The surface particle size of the pure and Gd-doped ferrite sample was approximately estimated to be between 22.23-34.26 nm, which is in close agreement with the crystallite size ( $D_{P-XRD}$ ) value found through P-XRD analysis (Scherrer's method) for the same sample. The observed average grain size proved the nanocrystalline structure of the prepared samples.



**Fig(2): FESEM Micrographs of Gd doped MnCd nanoferrites**

**Fig. 3. EDX photographs of pristine (Gd-0) and  $Gd^{3+}$ -doped (Gd-1- Gd-5) nano ferrite**

The purported chemical purity of all Gd-system-prepared materials is confirmed by the identified EDX spectrum, which only displays the peaks of Mn, Cd, Gd, iron Fe, and oxygen (O). from Fig(3).

**HRTEM ANALYSIS:** HRTEM is a characterization technique that is used to determine crystal structures. The images shows a lattice resolved image of the nanoferrites with a clear arrangement of atoms. The image has distinct lattice fringes that indicates a high degree of crystallinity. The interplanar spacing is measured to be approximately 0.25nm, corresponding to the (311) plane of the cubic spinel structure. The HRTEM image confirms the cubic spinel structure. They have a size range of approximately 22-26 nm and exhibit decreasing particle size behavior as the  $Gd^{3+}$  content increases.

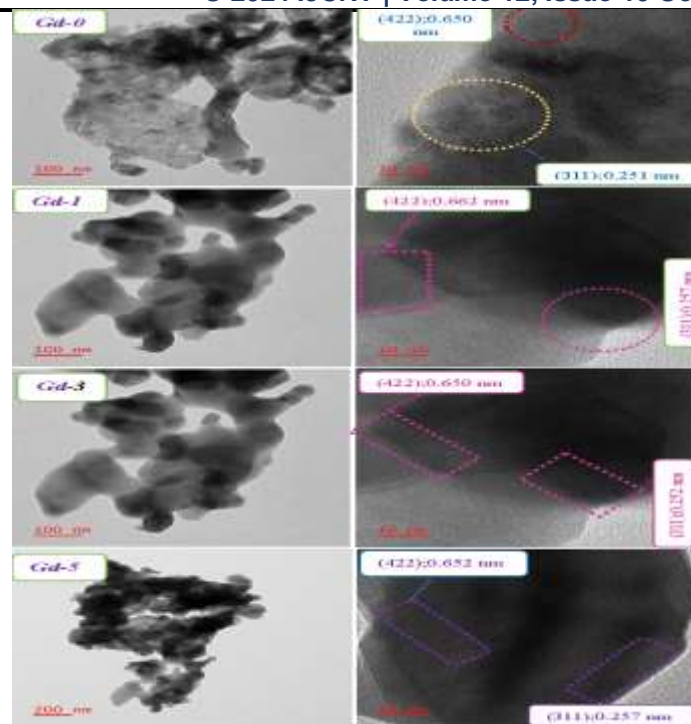


**Fig. 4. Transmission electron microscopy (TEM) micrographs of  $Mn_{0.7}Cd_{0.3}Gd_xFe_{2-x}O_4$  nanoparticles (a) Gd-0, (b) Gd-1, (c) Gd-3, (d) Gd-5** They have a size range of approximately 22-26 nm and exhibit decreasing particle size behavior as the  $Gd^{3+}$  content increases.

**SAED ANALYSIS:** It is a characterization technique used to study the crystal structure of materials. A diffraction pattern is produced from a selected area of the sample. The sharp spots in the diffraction pattern indicate a crystalline material and the concentric rings indicate a polycrystalline material. The SAED pattern indicates a cubic spinel structure. The below figure confirms the above analysis.

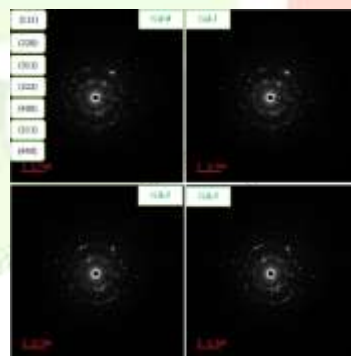


**Fig. 5. SAED patterns for  $Mn_{0.3}Cd_{0.7}Gd_xFe_{2-x}O_4$   $x = Gd-0, Gd-1, Gd-3, Gd-5$  nanoparticles**

**FTIR ANALYSIS:** This characterization technique involves measuring the absorption of infrared radiation by the nanoferrite samples. On analysis of FTIR spectrum, the chemical composition, crystal structure and surface properties and the Gd doping in the MnCd nanoferrites are known.

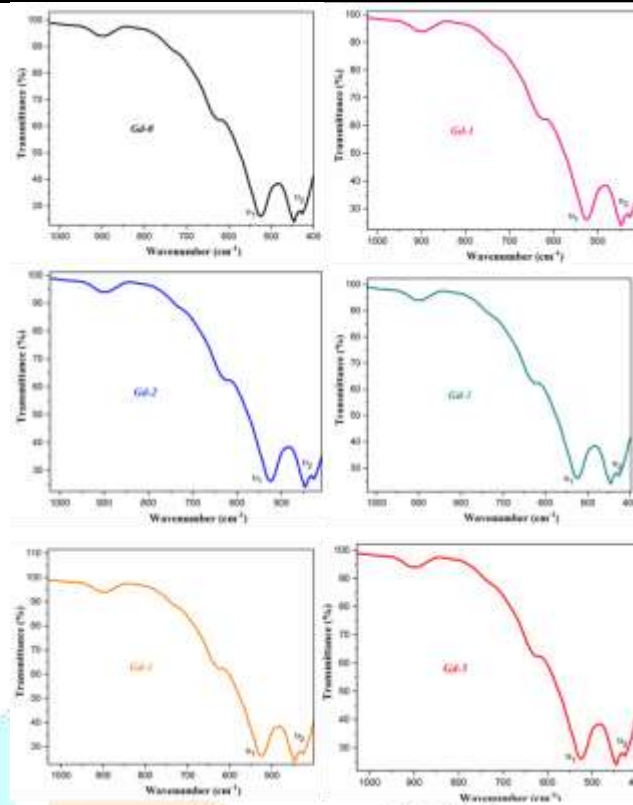


**Fig. 6 FTIR transmission spectra of  $Mn_{0.3}Cd_{0.7}Fe_{2-x}Gd_xO_4$  ( $x= Gd-0$  to  $Gd-5$ ) ferrite nanoparticles.**

The vibration of metal-oxygen group complexes in the octahedral B-site is responsible for the lower frequency bands  $\nu_2$   $cm^{-1}$ . Trivalent metal-oxygen ( $Fe^{3+}-O^{2-}$ ) bond stretching vibration in the tetrahedral A-site is associated with the higher frequency band  $\nu_1$   $cm^{-1}$ .

### Thermoelectric Power of Gadolinium-Doped Manganese Cadmium Nanoferrites

Thermoelectric materials have acquired significant interest due to their ability to convert heat into electrical energy. Among various thermoelectric materials, nanoferrites have emerged as promising candidates because of their unique electrical and magnetic properties. In particular, gadolinium-doped manganese cadmium nanoferrite (Gd-doped Mn-Cd nanoferrite) has shown potential due to its enhanced thermoelectric performance. This essay explores the thermoelectric power of Gd-doped Mn-Cd nanoferrite, discussing its synthesis, structural properties, and thermoelectric characteristics.

#### Synthesis and Structural Properties

Gadolinium-doped manganese cadmium nanoferrite is typically synthesized using the sol-gel auto-combustion method. This technique allows for the production of highly pure and homogenous nanoferrite particles. In a typical synthesis process, stoichiometric amounts of manganese nitrate, cadmium nitrate, gadolinium nitrate, and ferric nitrate are dissolved in distilled water. Citric acid is then added as a fuel, and the solution is heated until it undergoes auto-combustion, resulting in a fine powder of Gd-doped Mn-Cd nanoferrite.

The structural properties of the synthesized nanoferrite are characterized using techniques such as X-ray diffraction (XRD) and transmission electron microscopy (TEM). XRD patterns typically reveal a single-phase spinel structure with no secondary phases, indicating successful doping of gadolinium into the Mn-Cd ferrite lattice. TEM images show nanoparticles with an average size ranging from 10 to 30 nm, confirming the nanometric nature of the synthesized material. FESEM and EDAX analysis have confirmed the formation of the spinel structure of the synthesized compounds and the presence of the elements of the compound as considered. To study the thermoelectric properties of the samples of Gadolinium doped Manganese cadmium nanoferrites, the differential method involving Seebeck effect is employed and as mentioned in the above section of Introduction, the samples are made in the pellet form and is placed in a special arrangement of probes and much before placing the pellet between the electrodes the pellets are coated with silver paint and heated on a hot plate to have a better conductivity. The experiment is started

with the pure sample with concentration of  $x=0.000$  and adjusting the temperature values of hot and cold junctions so as to achieve a temperature difference of about 10K. The heating process is continued till the optimum temperature of the chosen sample of about 500K. The readings of the voltage developed due to the temperature gradient setup between the two electrodes is recorded during the cooling process. From the graphs of various compositions of the samples prepared plotted between Seebeck coefficient and Temperature shown in Fig (4), the transition temperature in each case is identified at the inflection point of the curve where the value of Seebeck coefficient starts to increase. At the transition temperature the dominant thermoelectric mechanism changes, thereby resulting in a significant change in the value of seebeck coefficient value. The sudden change in the value of Seebeck coefficient value indicates a phase transition from ferrimagnetic to paramagnetic phase. As mentioned earlier the energy band gap,  $E_g$  and the carrier concentration,  $n$ , is calculated using the equations (8) & (9) and from the table 2 the carrier concentration is decreasing for the doping concentrations of  $x=0.005, 0.015, 0.020, 0.025$  that proves beneficial in the context of optimizing magnetoresistance that is desirable for certain applications that include magnetic sensors, data storage in hard disk drives and magnetic RAM, helps in reducing thermal conductivity which can be beneficial for thermoelectric applications and even enhances spin dependent properties such as spin polarization.

Fig(4) Plots between Seebeck Coefficient (S) Vs Temperature, T for various dopant concentrations

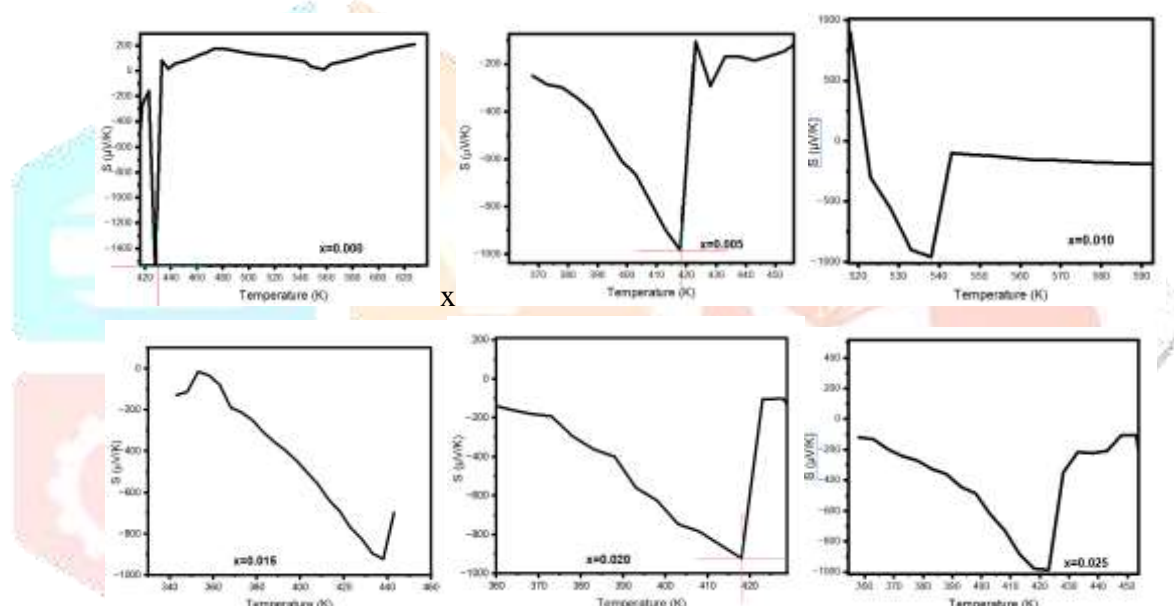


Table 2 : Values of Transition Temperature, Seebeck Coefficient, concentration of charge carriers, energy band gap with increase in doping concentration

S.No	Composition of the sample	Transition Temperature(K)	Seebeck Coefficient( $\mu\text{V/K}$ )	Concentration of the charge carriers( $\text{cm}^3$ )	Energy Band Gap( $E_g$ )eV
1	$\text{Mn}_{0.3}\text{Cd}_{0.7}\text{Gd}_0\text{Fe}_2\text{O}_4$	429.644	-1538.6401	$1.43 \times 10^{16}$	0.211
2	$\text{Mn}_{0.3}\text{Cd}_{0.7}\text{Gd}_{0.005}\text{Fe}_2\text{O}_4$	418.167	-985.3911	$5.03 \times 10^{15}$	0.264
3	$\text{Mn}_{0.3}\text{Cd}_{0.7}\text{Gd}_{0.010}\text{Fe}_2\text{O}_4$	538.315	-953.6483	$1.14 \times 10^{16}$	0.323
4	$\text{Mn}_{0.3}\text{Cd}_{0.7}\text{Gd}_{0.015}\text{Fe}_2\text{O}_4$	437.740	-913.1578	$4.65 \times 10^{15}$	0.256
5	$\text{Mn}_{0.3}\text{Cd}_{0.7}\text{Gd}_{0.020}\text{Fe}_2\text{O}_4$	418.244	-920.3162	$5.51 \times 10^{15}$	0.249
6	$\text{Mn}_{0.3}\text{Cd}_{0.7}\text{Gd}_{0.025}\text{Fe}_2\text{O}_4$	422.933	-974.4655	$4.23 \times 10^{15}$	0.263

	0.025 O <sub>4</sub>				
--	----------------------	--	--	--	--

Analysis on Transition temperature, Seebeck Coefficient, carrier concentration and energy band gap from the above Table 2: It is observed that at  $x = 0.000, 0.005$ ,  $E_g$  increases rapidly from 0.211 to 0.264 eV and the carrier concentration is found to decrease. This decrease in carrier concentration due to increase in the concentration of dopant is attributed to the electronic structure of the sample being modified due to compensation effects where Gd dopants might be compensating for existing defects or impurities. As the dopant concentration is increased i.e., for  $x = 0.015, 0.020$ ,  $E_g$  was increasing with increase in carrier concentration. Further for  $x = 0.010$ ,  $E_g$  attained a maximum value of 0.323 eV and carrier concentration increases indicating an increase in the carriers. At  $x = 0.025$ ,  $E_g$  increased with a decrease in carrier concentration.

It is to be noted that initial doping of rare earth metal ion  $Gd^{+3}$  reduces the charge carrier concentration and for moderate doping of  $x = 0.010$ , the charge carrier concentration increases and later on there is a decrease in the carrier concentration as dopant concentration is increased. The reason for this type of behavior is attaining a saturation value where the addition of dopant does not affect the charge carrier concentration.

From the above analysis the optimal Gd concentration for achieving the desired value of charge carrier concentration in nanoferrites is 0.010--0.015, where a balance between  $E_g$  and carrier concentration is achieved.

As the dopant concentration is increased,  $E_g$  is decreasing or like plateau due to the formation of secondary phases or changes in the electronic structure of the material.

It is to be further noted that increase in  $E_g$  indicates a wider band gap and decrease in carrier concentration that helps in improving optical and electrical properties.

Figure of Merit (ZT): It is a dimensionless quantity that represents the material's thermal performance.

The formula used to calculate ZT is

$$ZT = (S^2 \sigma T) / \kappa \text{ ----- (10)}$$

Where ZT is the figure of merit,

S is the Seebeck Coefficient,

$\sigma$  is the electrical conductivity,

T is the absolute temperature,

$\kappa$  is the Thermal Conductivity whose value is 0.08 cal/cm-K [20,21]

The value of ZT for optimal doping concentration of  $x = 0.010$  is determined and is found to be 0.83 which is considered relatively good.

Conclusion: The nano ferrites with the composition  $Mn_{0.3}Cd_{0.7}Gd_x Fe_{2-x} O_4$  with  $x = 0.000, 0.005, 0.010, 0.020, 0.025$  is synthesized using auto combustion citrate gel method and the structural, morphological analysis is carried out through characterization techniques that included P-XRD, FESEM, EDAX, TEM, SAED which confirmed the formation of spinel structure of the samples mentioned above with the values of lattice constant parameter, hopping lengths, particle size are found to be within the range of nanoparticles. Further as part of the study of electrical properties, thermoelectric power is

considered wherein the samples in the pellet form are experimented using differential procedure of seebeck effect. The values of Transition temperature at which the sample has a transition from n type to p type and the effects of increasing doping concentration on the seebeck coefficient and calculation of energy band gap and hence charge carrier concentration is carried. The combination of S and n trends suggests that the material's semiconductor behaviour is being tuned by the dopant  $Gd^{+3}$  with a transition from p type to n type behavior and a decrease in charge carrier concentration. The sample's electronic structure is being modified by the Gd doping, leading to a decrease in n. From the studies of Thermoelectric power it has been observed that the optimal doping concentration where the sample has required semiconducting nature is identified and the numerous applications include Thermoelectric generators that convert waste or dissipated heat into electric power this is suited for Industrial waste recovery, automotive exhaust heat recovery, Thermoelectric coolers used for CPUs, Medical devices, aerospace applications, sensors. And further studies can enhance the electrical properties.

#### References:

- [1] M.J.Iqbal, Z.Ahmad, T.Meydan, I.C.Nlebedim, Influence of Ni-Cr substitution on the magnetic and electrical properties of Mg ferrite nanomaterials. *Materials Research Bulletin* 47, 344-351, 2012
- [2] S.Paul, R.Patil, B.Chougule, DC electrical and thermoelectric power measurement studies of Ni-Mg-Zn-Co ferrites, *Journal of Magnetism and Magnetic Materials* 335, 109-113, 2015
- [3] E.Malicka, H.Duda, T.Gron, A.Gagor, S.Mazur, J.Krok-Kowalski, Thermoelectric power of  $CuCr_xV_ySe_4$  p-type spinel semiconductors, *Journal of Physics and chemistry of solids* 73, 262-268, 2012
- [4] S.Bachhav, R.Patil, P.Ahirrao, A.Patil, D.Patil, Microstructure and magnetic studies of Mg-Ni-Zn-Cu ferrites, *Materials Chemistry and Physics* 129, 1104-1109, 2011
- [5] V.D.Reddy, M.Malik, P.V.Reddy, Electrical Transport properties of Mn-Mg mixed ferrites, *Materials Science and Engineering B* 5, 295-301, 1991
- [6] N.Varalaxmi, K.Sivakumar, Structural, magnetic, DC-AC electrical conductivities and thermoelectric studies of  $MgCuZn$  ferrites for microinductor applications, *Materials Science and Engineering C* 33, 145-152, 2013
- [7] Farhadi, S., Pourzare, K., Sadeghinejad, S.: Simple preparation of ferromagnetic  $Co_3O_4$  nanoparticles by thermal dissociation of the  $[CoII(NH_3)_6](NO_3)_2$  complex at low temperature. *J. Nanostruct. Chem.* 3, 16 (2013)
- [8] Baba, P.D., Argentina, G.M., Courtney, W.E., Dionne, G.F., Temme, D.H.: Fabrication and properties of Microwave Lithium ferrites. *IEEE Trans. Magn.* 8, 83-94 (1972)
- [9] Gabal, M.A., Ata-Allah, S.S.: Effect of the diamagnetic substitution on the structural, electrical and magnetic properties of the cobalt ferrites. *Mater. Chem. Phys.* 85, 104-112 (2004)
- [10] Kawazoe, H., Ueda, K.: Transparent conductive oxides based on the spinel structure. *J. Am. Ceram. Soc.* 82, 3330-3336 (1999)
- [11] Venugopal Reddy, P., Sheshagiri rao, T.: X-ray studies on lithium-nickel and manganese-magnesium mixed ferrites. *J. Less Common Metals* 75, 255-1980 (1980)
- [12] Roy, P.K., Bera, J.: Effect of Mg substitution on electromagnetic properties of  $Ni_{0.25}Cu_{0.2}Zn_{0.55}Fe_2O_4$  ferrite prepared by auto combustion method. *J. Magn. Mater.* 298, 38-42 (2006)
- [13] Raghasudha, M., Ravinder, D., Veerasomaiah, P.: Magnetic properties of Cr-substituted Co-ferrite nanoparticles synthesized by citrate-gel auto combustion method. *J. Nanostruct. Chem.* 3, 63 (2013)

- [14] Lelis, M.F.F., Porto, A.O., Goncalves, C.M., Fabris, J.D.: Cation occupancy sites in synthetic Co-doped magnetites as determined with X-ray absorption (XAS) and Mossbauer spectroscopies. *J. Magn. Magn. Mater.* 278, 263–269 (2004)
- [15]. Al-Hilli, M.F., Li, S., Kassim, K.S.: Microstructure, electrical properties and Hall coefficient of europium doped Li–Ni ferrites. *Mater. Sci. Engg. B* 158, 1–6 (2009)
- [16] Liu, C., Lan, Z., Jiang, X., Yu, Z., Sun, K., Li, L., Liu, P.: Effects of sintering temperature and Bi<sub>2</sub>O<sub>3</sub> content on microstructure and magnetic properties of Li–Zn ferrites. *J. Magn. Magn. Mater.* 320, 1335–1339 (2008)
- [17]. Rodrigues, H.O., PiresJunior, G.F.M., Almeida, J.S., Sancho, E.O., Ferreira, A.C., Silva, M.A.S., Sombra, A.S.B.: Study of the structural, dielectric and magnetic properties of Bi<sub>2</sub>O<sub>3</sub> and PbO addition on BiFeO<sub>3</sub> ceramic matrix. *J. Phys. Chem. Solids* 71, 1329–1336 (2010)
- [18]. Ravi kumar, B., Ravinder, D.: TEP studies of Gd substituted Mn– Zn ferrites. *Mater. Lett.* 53, 441–445 (2002) Singh et al.,IDA study of magnetic and electronic properties of Gd doped Mn-Cg nanoferrites,20206
- [19]. Raghasudha, M., Ravinder, D., Veerasomaiah, P.: Characterization of nano-structured magnesium–chromium ferrites by Citratagel auto combustion method. *Adv. Mat. Lett.* 4, 910–916 (2013) Kumar et al., DFT (Density Functional Theory) study of Gd doped Mn-Cd nanoferrites,2019
- [20] Raghasudha, M., Ravinder, D., Veerasomaiah, P.: Thermoelectric power studies of Co–Cr nano ferrites. *J. Alloys Comp.* 604, 276–280 (2014) K.M.Batoo et al., Thermal and Electrical properties of manganese cadmium nanoferrites, *Journal of Alloys and Compounds*, vol.649, pp.1231-1236,2015
- [21] .S.Thermoelectric generators,Industrial waste recovery,automotive exhaust heat recovery,Thermoelectric coolers used for CPUs,Medical devices,aerospace applications,sensors. Bellad et al.,Thermal conductivity of gadolinium doped nanoferrites,*Materials Research Express*,vol.6,no.10,p.1057033,2019